2026 10th Scientific School Dynamics of Complex Networks and their Applications (DCNA) | 979-8-3195-2599-4/26/$31.00 ©2026 IEEE | DOI: 10.1109/DCNA72004.2026.11733398

Identification of the epileptogenic zone from long-range temporal correlations of interictal sEEG activity using machine learning methods

Nikita Konyakhin
Plekhanov Russian University of Economics
Moscow, Russia
konyahin.n@edu.rea.ru

Pavel Chirkin
Plekhanov Russian University of Economics
Moscow, Russia
chirkin_07.p@mail.ru

Alexander Kuc
Plekhanov Russian University of Economics
Moscow, Russia
kuts.ak@rea.ru

***Abstract*—An automated approach for identifying stereo-electroencephalography (sEEG) channels belonging to the clinically defined epileptic seizure onset zone, based on interictal activity, is proposed. The study used data from 23 patients with focal epilepsy, from which a sample of 1974 bipolar channels was formed, including 235 focal and 1739 non-focal channels. As interpretable features, long-range temporal correlation measures were applied, quantified by detrended fluctuation analysis (DFA) independently in eight frequency bands from 1 to 120 Hz. Logistic regression, random forest, and support vector machines with linear and radial basis function kernels were compared. Under 5-fold cross-validation with patient-wise grouping, the best result was achieved by a linear SVM on eight DFA features (ROC-AUC = 0.713 $\pm$ 0.046). A comparable result was obtained using the four most informative bands (ROC-AUC = 0.711 $\pm$ 0.042). The 1–4 Hz and 70–100 Hz bands proved to be the most consistently informative.**

***Index Terms*—stereo-EEG, epileptogenic zone, long-range temporal correlations, detrended fluctuation analysis, machine learning, support vector machine**

I. Introduction

Electroencephalographic methods are widely used to study disturbances of brain dynamics in various neurological and psychoneurological conditions. The analysis of the spatio-temporal organization of neural activity is of interest not only in epilepsy but also in tasks such as post-stroke neurorehabilitation [1], the study of depressive disorder [2], [3], autism spectrum disorders [4], and other conditions accompanied by changes in the functional organization of brain networks. This creates a need for quantitative biomarkers that can be computed directly from neurophysiological data and are comparable across patients.

Epilepsy is one of the most common neurological disorders: according to World Health Organization estimates, it affects approximately 50 million people worldwide [5]. Of particular interest is the study of the mechanisms underlying pathological neural activity [6]. In a simplified view, the epileptic process can be regarded as a state of pathological synchronization of neuronal ensembles. This approach makes it possible to relate the observed changes in neurophysiological signals to the dynamics of interacting brain elements and to investigate the mechanisms underlying the emergence of pathological synchronization using not only experimental data but also theoretical models [7], [8]. In particular, models of coupled oscillators make it possible to study how changes in the dynamical characteristics of individual nodes can contribute to the formation of a pathologically synchronized state [9].

However, translating these concepts into clinical practice is considerably more difficult. When examining patients with drug-resistant focal epilepsy [10], the epileptologist faces two principal tasks: detecting the onset of an epileptic seizure from long-term EEG recordings [11], and localizing the epileptogenic zone, which determines the feasibility and extent of surgical intervention [12]. Stereo-electroencephalography (sEEG), which enables the recording of activity from deep brain structures, is widely used to address the second task [13], [14]. The use of interictal activity potentially allows the pathological features of neural dynamics to be evaluated without the need to wait for a spontaneous seizure. In particular, interictal high-frequency oscillations [15] and abnormal temporal dynamics of seizure-free intracranial recordings [16] have been shown to mark epileptogenic cortex.

An important requirement for automated methods supporting clinical decision-making is not only high discriminative ability but also the interpretability of the features used [17]. For clinical application, characteristics with a clear physiological and mathematical interpretation are preferable, as they make it possible to explain why a particular channel is assigned to a potentially pathological region [18], [19]. One such feature is long-range temporal correlations (LRTC) [20], quantified using detrended fluctuation analysis (DFA) [21], [22]. This method makes it possible to quantitatively describe the scale-invariant structure of temporal dynamics and to examine its dependence on frequency band, in line with multiscale approaches to biomedical signal characterization [23].

The aim of the present study is to evaluate the feasibility of

This work is supported from the Russian Science Foundation (project 23-71-30010)

Authorized licensed use limited to: Kant Baltic Federal Univ. Downloaded on October 23,2026 at 15:24:09 UTC from IEEE Xplore. Restrictions apply.

automated classification of focal and non-focal sEEG channels based on multiband DFA features of interictal activity, and to identify the most effective yet interpretable classifier.

II. Materials and methods

A. Dataset and clinical labeling

Data from 23 patients with focal drug-resistant epilepsy who underwent long-term invasive sEEG monitoring and for whom clinical documentation of epileptogenic zone localization was available were analyzed. The data were obtained at the Pirogov National Medical and Surgical Center. For all patients, sEEG recordings were converted to a bipolar montage.

The clinical documentation contained only positively identified focal contact ranges for each electrode. A bipolar channel was labeled as focal only if both of its contacts were located within the same continuous focal range documented for that electrode. Channels for which only one contact fell within a documented focal range, or in which both contacts belonged to two non-adjacent focal sub-ranges of the same electrode, were considered ambiguous and excluded.

The resulting dataset comprised 1974 bipolar channels: 235 focal and 1739 non-focal (focal class proportion 11.9%). The classification task was therefore characterized by pronounced class imbalance, and patient-wise data grouping was essential to prevent information leakage between training and validation.

B. sEEG recording and preprocessing

For each patient, a 15-minute interictal sEEG segment sampled at 256 Hz was analyzed. To eliminate noise, volume conduction, and distant reference effects, the channels were converted into a spatially localized bipolar configuration. Bipolar channels were constructed sequentially along each electrode shaft by subtracting the signal of contact $i+1$ from the signal of contact i:

$$S_{\text{bipolar},\,i}(t) = S_i(t) - S_{i+1}(t) \tag{1}$$

Channels originating from scalp electrodes or contacts not associated with the brain were automatically excluded using regular-expression-based analysis of electrode labels.

The resulting signal was divided into five non-overlapping 180-second windows. Each windowed signal was band-pass filtered using a finite-impulse-response (FIR) filter, and its amplitude envelope was obtained using the Hilbert transform.

C. Multiband FIR filtering and envelope extraction

To characterize frequency-dependent dynamics, taking into account that different spectral components of a complex signal may exhibit distinct dynamical and synchronization properties [8], eight spectral bands were formed: 1–4, 4–8, 8–13, 13–30, 30–50, 50–70, 70–100, and 100–120 Hz. For each band, DFA was computed independently in each of the five 180-second windows and then averaged across windows, yielding eight DFA features per bipolar channel. Additionally, a single-band baseline variant of 60–63 Hz was evaluated.

D. Detrended fluctuation analysis

Filtering was performed on the full 15-minute signal prior to window segmentation. Hamming-windowed finite-impulse-response (FIR) band-pass filters were applied using two-pass, zero-phase forward-backward filtering (filtfilt) to prevent phase distortion. The filter order N was adapted based on the lower cutoff frequency f_{hp} and the sampling frequency f_s:

$$N = \left\lfloor \min\left(\frac{7.0}{f_{hp}},\, 3.0\right) \cdot f_s \right\rfloor \tag{2}$$

After band-pass filtering, the instantaneous amplitude envelope $A(t)$ was computed using the analytic signal obtained from the Hilbert transform:

$$z(t) = x(t) + i \cdot \mathcal{H}\left\{x(t)\right\} \tag{3}$$

$$A(t) = |z(t)| = \sqrt{x^2(t) + \mathcal{H}\left\{x(t)\right\}^2} \tag{4}$$

Extracting the envelope from the continuous 15-minute recording eliminated the boundary transient artifacts that typically arise when filtering short windowed segments.

An integrated profile was then constructed for each signal:

$$Y(k) = \sum_{t=1}^{k} \left[A(t) - \langle A \rangle\right], \quad k = 1, \ldots, N \tag{5}$$

For a given scale s, the profile was divided into segments of length s with 50% overlap. Linear detrending was performed within each segment. The fluctuation for segment ν was defined as:

$$F^2(\nu, s) = \frac{1}{s} \sum_{k=1}^{s} \left\{ Y\left[(\nu - 1)s + k\right] - p_\nu^{(1)}(k) \right\}^2 \tag{6}$$

The averaged fluctuation function was then calculated:

$$F(s) = \left\{ \frac{1}{2N_s} \sum_{\nu=1}^{2N_s} F^2(\nu, s) \right\}^{1/2} \tag{7}$$

Under power-law scaling $F(s) \sim s^{\mu}$, the DFA exponent μ was estimated as the slope of the linear regression of $\log F(s)$ on $\log s$. A value of $\mu = 0.5$ corresponds to uncorrelated dynamics, whereas $\mu > 0.5$ indicates persistent long-range temporal correlations.

E. Machine learning and validation

Four classifiers were compared: logistic regression, random forest, and support vector machines (SVM) with linear and RBF kernels — all using balanced class weighting to compensate for the imbalance between the focal and non-focal classes (≈1:7.4). The SVMs were trained within a pipeline with feature standardization fitted only on the training portion of each fold. Validation was performed using 5-fold StratifiedGroupKFold with patient-wise grouping, so that channels from the same patient never appeared simultaneously

Authorized licensed use limited to: Kant Baltic Federal Univ. Downloaded on October 23,2026 at 15:24:09 UTC from IEEE Xplore. Restrictions apply.

in the training and validation portions of a given fold. The resulting metrics — ROC-AUC, PR-AUC for the focal class, precision, and recall — were computed at each model's native decision threshold and averaged across the five folds. Permutation feature importance (scoring metric: ROC-AUC, 30 repeats), computed on the validation channels of each fold and averaged across folds, was used to assess the contribution of individual frequency bands for logistic regression and linear SVM. Top-N features were selected using only the training data, via nested validation with patient-wise grouping, to avoid information leakage into the validation folds.

III. Results

Table I compares the tested configurations on the set of eight DFA bands together with the single-band baseline variant. Linear SVM using the set of eight bands achieved the highest mean ROC-AUC (0.713) among the tested configurations — numerically higher than logistic regression on the same features (0.699) and than the RBF-kernel SVM (0.648). Restricting the linear SVM to the four most important bands preserved essentially the same ROC-AUC value (0.711), indicating that most of the discriminative information is concentrated in a subset of bands.

TABLE I
Comparison of Models (Mean ± Standard Deviation over 5 Patient-Grouped Folds, Native Decision Threshold)

Model	ROC-AUC	PR-AUC	Prec. (focal)	Rec. (focal)
LogReg, 60–63 Hz	.708±.063	.277±.046	.151±.025	.830±.158
LogReg, 8 bands	.699±.071	.281±.080	.220±.058	.556±.174
SVM-lin, 8 bands	**.713±.046**	**.298±.049**	.251±.067	.587±.198
SVM-RBF, 8 bands	.648±.060	.252±.065	.234±.055	.520±.188
SVM-lin, top-4	.711±.042	.286±.042	.241±.059	.570±.200

Permutation feature importance (Fig. 1) shows an uneven contribution of the bands for the linear SVM: the 1–4 Hz and 70–100 Hz bands proved to be the most consistently important. This is consistent with the known role of high-frequency activity as an interictal marker of epileptogenic tissue [15] and with the importance of low-frequency and high-frequency spectral features revealed by interpretability analysis of deep learning models for epileptic EEG [19].

The evaluation focused on the discriminative ability of the multiband DFA features and on determining the influence of continuous signal preprocessing and spatial postprocessing on classification accuracy.

IV. Conclusion

A linear support vector machine trained on eight band-averaged DFA features computed from interictal sEEG, under patient-grouped cross-validation, achieved a mean ROC-AUC of 0.713 ± 0.046, demonstrating good discriminative ability between focal and presumed non-focal sEEG channels; the 1–4 Hz and 70–100 Hz bands provided the most consistent contribution.

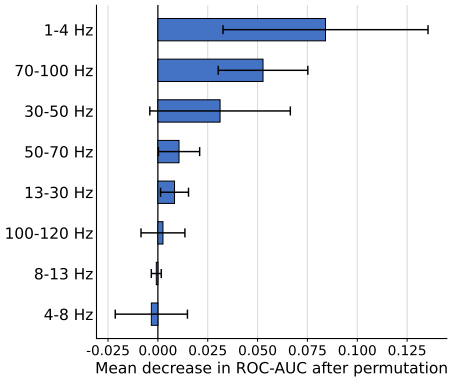


Fig. 1. Permutation-based importance of band-averaged DFA features for the linear SVM. Bars show the mean decrease in ROC-AUC after permuting a feature; error bars reflect variability across the five patient-grouped validation folds.

Future work will aim to extend the same DFA feature-extraction methodology to pre-ictal sEEG segments and to explore the possibility of unsupervised clustering of the DFA feature space as an additional analysis that does not require prior class labeling.

Disrupted long-range temporal correlations of high-frequency background activity serve as a reliable biomarker of localized cortical pathology, representing a valuable tool for automated mapping in epilepsy.

References

[1] V. Grubov, A. Badarin, N. Schukovsky, and A. Kiselev, "Brain-computer interface for post-stroke rehabilitation," *Cybernetics and physics*, vol. 8, no. 4, pp. 251–256, 2019.

[2] A. N. Pisarchik, A. V. Andreev, S. A. Kurkin, D. Stoyanov, A. A. Badarin, R. Paunova, and A. E. Hramov, "Topology switching during window thresholding fmri-based functional networks of patients with major depressive disorder: Consensus network approach," *Chaos: An Interdisciplinary Journal of Nonlinear Science*, vol. 33, no. 9, 2023.

[3] A. V. Andreev, S. A. Kurkin, D. Stoyanov, A. A. Badarin, R. Paunova, and A. E. Hramov, "Toward interpretability of machine learning methods for the classification of patients with major depressive disorder based on functional network measures," *Chaos: An Interdisciplinary Journal of Nonlinear Science*, vol. 33, no. 6, 2023.

[4] M. S. Kabir, S. Kurkin, G. Portnova, O. Martynova, Z. Wang, and A. Hramov, "Contrastive machine learning reveals in eeg resting-state network salient features specific to autism spectrum disorder," *Chaos, Solitons & Fractals*, vol. 185, p. 115123, 2024.

[5] A. Pitkänen, W. Löscher, A. Vezzani, A. J. Becker, M. Simonato, K. Lukasiuk, O. Gröhn, J. P. Bankstahl, A. Friedman, E. Aronica *et al.*, "Advances in the development of biomarkers for epilepsy," *The Lancet Neurology*, vol. 15, no. 8, pp. 843–856, 2016.

[6] C. P. Lisgaras, L. M. De La Prida, E. Bertram, M. Cunningham, D. Henshall, A. A. Liu, V. Gnatkovsky, S. Balestrini, M. De Curtis, A. S. Galanopoulou *et al.*, "The role of electroencephalography in epilepsy research—from seizures to interictal activity and comorbidities," *Epilepsia*, vol. 66, no. 5, pp. 1374–1393, 2025.

[7] A. E. Hramov, A. A. Koronovskii, and O. I. Moskalenko, "Are generalized synchronization and noise-induced synchronization identical types of synchronous behavior of chaotic oscillators?" *Physics Letters A*, vol. 354, no. 5-6, pp. 423–427, 2006.

[8] A. E. Hramov, A. A. Koronovskii, M. K. Kurovskaya, and O. I. Moskalenko, "Synchronization of spectral components and its regularities in chaotic dynamical systems," *Physical Review E—Statistical, Nonlinear, and Soft Matter Physics*, vol. 71, no. 5, p. 056204, 2005.

Authorized licensed use limited to: Kant Baltic Federal Univ. Downloaded on October 23,2026 at 15:24:09 UTC from IEEE Xplore. Restrictions apply.

[9] A. V. Andreev, V. A. Maksimenko, A. N. Pisarchik, and A. E. Hramov, "Synchronization of interacted spiking neuronal networks with inhibitory coupling," *Chaos, Solitons & Fractals*, vol. 146, p. 110812, 2021.
[10] P. Kwan, A. Arzimanoglou, A. T. Berg, M. J. Brodie, W. Allen Hauser, G. Mathern, S. L. Moshé, E. Perucca, S. Wiebe, and J. French, "Definition of drug resistant epilepsy: consensus proposal by the ad hoc task force of the ILAE commission on therapeutic strategies," *Epilepsia*, vol. 51, no. 6, pp. 1069–1077, 2010.
[11] V. V. Grubov, S. I. Nazarikov, S. A. Kurkin, N. P. Utyashev, D. A. Andrikov, O. E. Karpov, and A. E. Hramov, "Two-stage approach with combination of outlier detection method and deep learning enhances automatic epileptic seizure detection," *IEEE Access*, vol. 12, pp. 122 168–122 182, 2024.
[12] F. Rosenow and H. Lüders, "Presurgical evaluation of epilepsy," *Brain*, vol. 124, no. 9, pp. 1683–1700, 2001.
[13] J. A. Gonzalez-Martinez, "The stereo-electroencephalography: the epileptogenic zone," *Journal of Clinical Neurophysiology*, vol. 33, no. 6, pp. 522–529, 2016.
[14] F. Bartolomei, P. Chauvel, and F. Wendling, "Epileptogenicity of brain structures in human temporal lobe epilepsy: a quantified study from intracerebral EEG," *Brain*, vol. 131, no. 7, pp. 1818–1830, 2008.
[15] J. Jacobs, R. Staba, E. Asano, H. Otsubo, J. Wu, M. Zijlmans, I. Mohamed, P. Kahane, F. Dubeau, V. Navarro, and J. Gotman, "High-frequency oscillations (HFOs) in clinical epilepsy," *Progress in Neurobiology*, vol. 98, no. 3, pp. 302–315, 2012.
[16] S. Monto, S. Vanhatalo, M. D. Holmes, and J. M. Palva, "Epileptogenic neocortical networks are revealed by abnormal temporal dynamics in seizure-free subdural EEG," *Cerebral Cortex*, vol. 17, no. 6, pp. 1386–1393, 2007.
[17] O. E. Karpov, V. V. Grubov, V. A. Maksimenko, S. A. Kurkin, N. M. Smirnov, N. P. Utyashev, D. A. Andrikov, N. N. Shusharina, and A. E. Hramov, "Extreme value theory inspires explainable machine learning approach for seizure detection," *Scientific Reports*, vol. 12, no. 1, p. 11474, 2022.
[18] O. E. Karpov, S. Afinogenov, V. V. Grubov, V. Maksimenko, S. Korchagin, N. Utyashev, and A. E. Hramov, "Detecting epileptic seizures using machine learning and interpretable features of human eeg," *The European Physical Journal Special Topics*, vol. 232, no. 5, pp. 673–682, 2023.
[19] V. V. Grubov, O. E. Karpov, S. I. Nazarikov, S. A. Kurkin, N. P. Utyashev, D. A. Andrikov, and A. E. Hramov, "An interpretability framework for convolutional neural network-based electroencephalography analysis discovers new spatial and spectral epileptic biomarkers," *International Journal of Neural Systems*, p. 2650033, 2026.
[20] K. Linkenkaer-Hansen, V. V. Nikouline, J. M. Palva, and R. J. Ilmoniemi, "Long-range temporal correlations and scaling behavior in human brain oscillations," *The Journal of neuroscience*, vol. 21, no. 4, pp. 1370–1377, 2001.
[21] C.-K. Peng, S. Havlin, H. E. Stanley, and A. L. Goldberger, "Quantification of scaling exponents and crossover phenomena in nonstationary heartbeat time series," *Chaos*, vol. 5, no. 1, pp. 82–87, 1995.
[22] R. Hardstone, S.-S. Poil, G. Schiavone, R. Jansen, V. V. Nikulin, H. D. Mansvelder, and K. Linkenkaer-Hansen, "Detrended fluctuation analysis: a scale-free view on neuronal oscillations," *Frontiers in physiology*, vol. 3, p. 450, 2012.
[23] L. Kralj, S. Kurkin, H. Lenasi, A. Pavlov, A. Stožer, A. E. Hramov, M. Perc, and M. Gosak, "Wavelet analysis in biomedical research: A versatile tool for multiscale signal characterization and functional connectivity analysis," *Physics of Life Reviews*, vol. 59, pp. 19–47, 2026.

Authorized licensed use limited to: Kant Baltic Federal Univ. Downloaded on October 23,2026 at 15:24:09 UTC from IEEE Xplore. Restrictions apply.